Light absorption properties of laboratory generated tar ball particles

A. Hoffer[1], A. Tóth[2], I. Nyirő-Kósa[1], M. Pósfai[2], A. Gelencsér[1,2]

[1]{MTA-PE Air Chemistry Research Group, Veszprém, P.O. Box 158, H-8201, Hungary}

[2]{Department of Earth and Environmental Sciences, University of Pannonia, Veszprém, P.O. Box 158, H-8201, Hungary}

Correspondence to: A. Gelencsér (gelencs@almos.uni-pannon.hu)

Abstract

Tar balls (TBs) are a specific particle type which is abundant in the global troposphere, in particular in biomass smoke plumes. These particles belong to the family of atmospheric brown carbon (BrC) which can absorb light in the visible range of the solar spectrum. Albeit TBs are typically present as individual particles in biomass smoke plumes, their absorption properties have been only indirectly inferred from field observations or calculations based on their electron energy-loss spectra. This is because in biomass smoke TBs coexist with various other particle types (e.g. organic particles with inorganic inclusions and soot, the latter is emitted mainly during flaming conditions) from which they cannot be physically separated; thus, a direct experimental determination of their absorption properties is not feasible. Very recently we have demonstrated that TBs can be generated in the laboratory from droplets of wood tar that resemble atmospheric TBs in all of their observed properties. As a follow-up study we have installed on-line instruments to our laboratory set-up generating pure TB particles to measure the absorption and scattering, as well as size distribution of the particles. In addition, samples were collected for transmission electron microscopy (TEM) and total carbon (TC) analysis. The effects of experimental parameters were also studied. The mass absorption coefficients of the laboratory generated TBs were found to be in the range of 0.8–3.0 m^2g^{-1} at 550 nm, with absorption Ångström exponents (AAE) between 2.7 and 3.4 (average 2.9) in the wavelength range 467–652 nm. The refractive index of TBs as derived from Mie calculations was about 1.84−0.21i at 550 nm. In the brown carbon continuum these values fall closer to those of soot than to other light-absorbing species such as humic-like

substances (HULIS). Considering the abundance of TBs in biomass smoke and the global magnitude of biomass burning emissions, these findings may have substantial influence on the understanding of global radiative energy fluxes.

1 Introduction

Tar balls (TBs) are ubiquitous in the global troposphere and represent a peculiar particle type emitted from biomass burning. The contribution of TBs to the number concentration of particles could be as high as 80% in the vicinity of biomass burning sources (Pósfai et al., 2003), while it was in the range of 6–14% away from the sources (Adachi et al., 2011), as observed using TEM. At a site that represents regional background conditions (K-puszta) the abundance of TBs varied from 0 to 40% depending on the season and time of sampling (Pósfai et al., 2004). Even over the Himalaya TB particles accounted for 3% of all observed particles (Cong et al., 2009). Near the Arctic, in Hyytiälä during a pollution episode 1–4% of the particles were identified as TBs (Niemi et al., 2006). Tar balls can be readily identified by transmission electron microscopy (TEM) by their morphology, chemical composition, and amorphous structure. TBs are homogeneous and spherical particles that can withstand the high-energy electron beam of the TEM. They are most often present in external mixture, i.e. as individual standalone particles. Their sizes range from 30 to 500 nm in geometric diameter as determined by TEM (Pósfai et al., 2004; Cong et al., 2009; Adachi and Buseck 2010; Fu et al., 2012; China et al., 2013). Very recently we have demonstrated that TBs can be generated in the laboratory from droplets of wood tar that resemble atmospheric TBs in all of their observed properties (Tóth et al., 2014). These particles belong to the family of atmospheric brown carbon (BrC) which can absorb light in the visible range of the solar spectrum (Andreae and Gelencsér 2006). Chung and co-workers (2012) have estimated that the global contribution of BrC to light absorption may be as high as 20% at 550 nm. Given that the estimated contribution of humic-like substances (HULIS) to solar absorption can be only few per cent at 500 nm (Hoffer et al., 2006), a substantial fraction of BrC absorption may be attributed to TBs. So far a direct experimental determination of absorption properties of TBs has not been feasible because in biomass smoke TBs coexist with various other particle types from which they cannot be separated. Thus, their absorption properties have been so far only indirectly inferred from field observations (Hand et al., 2004; Chakrabarty et al., 2010) or calculations based on their dielectric functions obtained from electron energy-loss spectrometry (Alexander et al., 2008).

Hand and co-workers (2004) were the first to estimate the optical properties of TB by measuring the optical properties of ambient particles emitted from biomass burning during the YACS (Yosemite Aerosol Characterization Study) conducted from July to September 2002 in the western United States. The derived (estimated from OC/EC and scattering data) ensemble complex index of refraction of TBs was found to be 1.56−0.02i at 632 nm, indicating that the TBs do absorb light. The difference between the measured absorption between 370 nm and 880 nm was the highest in periods when TBs were the predominant particle type, suggesting that the absorption Ångström exponent (AAE) of TB was different from 1. Back-trajectory analyses showed that the particles measured were affected by long-range transport, thus the residence time of the particles allowed photochemical and ageing processes to take effect. These effects can be observed on the distribution of the elements in individual TB particles. Whereas carbon and nitrogen were homogenously distributed over the entire particle volume, the abundance of oxygen was strongly enhanced in the ~30 nm outmost shell of the particles. Since these particles were affected by atmospheric processing, some of their properties might be different from those of the freshly emitted TB particles.

Alexander and co-workers (2008) investigated individual particles ("carbon spheres") from ambient aerosols collected above the Yellow Sea during the Asian Pacific Regional Aerosol Characterization Experiment (ACE-Asia). The morphological properties (size, structure, and mixing state) of the carbon spheres observed by TEM were similar to those characteristic of TB particles. The refractive indices of individual carbon spheres were derived from theoretical calculations based on electron energy-loss spectra and were found to be centred around 1.67−0.27i at 550 nm. The authors also calculated the wavelength dependence of the absorption and found AAE of 1.5 which is not much different from that reported for BC (Schnaiter et al., 2003; Moosmüller et al, 2009). The derived mass absorption coefficients of the carbon spheres were in the range of 3.6–4.1 m^2g^{-1}, almost as high as those of BC (4.3–4.8 m^2g^{-1}) (Alexander et al., 2008).

Chakrabarty and co-workers (2010) measured the optical properties of tar balls from smoldering combustion of Ponderosa pine and Alaskan Pine duffs in the laboratory. They found the index of refraction of TB particles similar to those of humic-like substances (Hoffer et al., 2006). The wavelength dependent absorption Ångström exponents were split into 2.3–2.8 and 4.2–6.4 in the spectral range of 532–780 nm and 405–532 nm, respectively. The TB particles were almost spherical, having a carbon-to-oxygen ratio of about 6, as determined by SEM-EDX.

The absorption properties of BrC including TBs are very important in regional and global modelling of the radiative budget, as well as in interpreting satellite-based radiation measurements. In spite of being an abundant particle type among BrC particles, TBs have so far eluded direct measurements of their optical properties, since they always coexist with other particle types and UV-absorbing gaseous species in biomass smoke. By measuring pure TB particles in the laboratory without the concurrent presence of other combustion particles, we have directly obtained the optical properties of TBs for the first time in aerosol science. In this paper we report the fundamental optical properties of laboratory generated TBs generated under different conditions.

2 Experimental

For particle generation liquid tar was produced by dry distillation of wood, as described in our previous paper (Tóth et al., 2014). Briefly, dry European turkey oak wood (Quercus cerris) chops (25 × 10 × 10 mm) were placed in a Kjeldahl flask (100 mL) fixed above a Bunsen burner in a slightly down-tilted position. The liquid condensate produced during the pyrolysis in the Kjeldahl flask was collected in a 40 mL vial in which it separated into “oily” and "aqueous" phases (Maschio et al., 1992). Since the chemical compositions of the aqueous and the oily phase obviously differ, the two phases were separated and investigated separately. Both phases were aged further on a ~300°C plate to concentrate the solutions. The concentrates were taken up with high purity methanol (J.T. Baker, HPLC Gradient) and used for particle generation as described in the next paragraph. The concentrations of solutions used for particle generation were 1–3 g L^{-1}.

A modified experimental setup similar to that used in previous experiments (Tóth et al., 2014) was applied for particle generation (Figure 1). In order to maintain the concentration of the generated particles constant for a longer time that is necessary for measuring the size distribution and optical properties of the particles, particles were generated with an ultrasonic atomizer. The production of tar droplets from their solution in methanol was performed in a plastic flask placed above the ultrasonic nebulizer (1.6 MHz, Exo Terra Fogger, PT2080, Rolf C. Hagen Corp.), held in a water bath at room temperature. The nebulizer flask was continuously rinsed with purified nitrogen (Messer, purity 99.5 %) at a flow rate of 0.100 L min^{-1}. The generated droplets were passed through a glass tube of 300 mm length (id=9 mm) heated directly with a tube furnace (Carbolite, MTF 10/25/130). The temperature of the heated zone (30 mm isotherm zone) was set in the experiments between 500 and 800°C. The

residence time of the particles in the heated zone was about 1.15 s. After leaving the heated zone the nitrogen flow was mixed with dry filtered air at a flow rate of ~30 L min^{-1}, then passed through a buffer volume of 10.75 L (residence time ~22 s). A PM1 cyclone (SCC 2.229, BGI Inc.) was deployed at the outlet of the system to remove the large particles (the calculated cut-off was ~500 nm aerodynamic diameter) from the gas stream. The measurements of the optical parameters (scattering and absorption) and the size distribution as well as the aerosol sampling were performed in a single setup. The light absorption coefficients were measured with a CLAP (Continuous Light Absorption Photometer) at 3 different wavelengths (467, 528, 652 nm). The light scattering coefficients were measured with a TSI 3563 nephelometer at 450, 550, 700 nm (Anderson et al., 1996). The data were recorded with a time resolution of 5 s, the raw light absorption and scattering data were corrected according to Bond et al. (1999), and Ogren (2010) and Anderson and Ogren (1998), respectively. All data were also corrected for standard temperature and pressure. The absorption Ångström exponents of the particles were calculated from the measured and corrected absorption coefficient for the wavelength range between 467 and 652 nm with the equation (Moosemüller et al., 2011):

$$AAE = -\ln(A_{467}/A_{652}) / \ln(467/652),$$

where A_{467} and A_{652} are the absorbances measured at the two different wavelengths.

The size distribution was measured in the range of 7–800 nm with a Differential Mobility Particle Sizer (DMPS), constructed at the University of Helsinki.

The generated particles were collected on Whatman QMA quartz filters (pre-baked at 680°C for 6 hours). The elemental composition (CHNS) of the particles on filters was measured by elemental analyser (EuroVector EA3000). In certain cases the particles were collected on TEM grids (lacey Formvar/carbon TEM copper grid of 200 mesh, Ted Pella Inc., USA) fixed on 13.1 mm spots of quartz filters placed in the filter holder that were used for sampling for elemental analysis as well.

The morphologies of the particles were studied in bright-field TEM images obtained using a Philips CM20 TEM operated at 200 kV accelerating voltage. The possible presence of an internal structure was checked in high-resolution electron micrographs and in selected-area electron diffraction patterns. The electron microscope was equipped with an ultra-thin-window Bruker Quantax X-ray detector that allowed the energy-dispersive X-ray analysis

(EDS) of the elemental compositions of individual particles. Spectra were acquired for 60 s, with the diameter of electron beam adjusted to include the entire individual TB particles.

3 Results

3.1 Morphology, elemental composition and structure of the generated particles

Two samples were collected for TEM analysis to investigate the morphology and elemental composition of the generated particles, one representing the particles generated from the aqueous phase of the tar, whereas the other was collected from the oily phase. In both cases the oven temperature was set to 650°C, the flows and other experimental parameters were similar to those applied for samples collected for TC analysis.

As it can be observed in Figure 2, the particles generated from the aqueous phase were spherical. From the oily phase more irregularly shaped particles with oval two-dimensional outlines were produced, indicating that in the latter case the particles were not perfectly solid at the time of collection. It was observed during the TEM analysis that all of the generated particles can withstand the high-energy electron beam of the instrument: they did not evaporate or shrink while exposed to the electron beam.

The observed sizes of the particles vary widely (up to ~360 nm in diameter), the number size distribution peaks at ~100 nm as determined from the TEM images. Bimodal number size distribution was obtained from the DMPS measurements for the particles produced from both the aqueous and oily phase of the tar (Figure 3). For the particles aged at 650°C the two modes are centred around 20–40 and 100–140 nm. The number size distributions of nigrosin and the blank (pure methanol) are unimodal peaking at 117 and 41 nm, respectively. Nevertheless, in cases when the ageing temperature was higher than 500°C the mass and volume of the particles are dominated by the larger particles: at least 86% and 70 % of the total mass is represented by the larger particle mode in the case of the aqueous and oily samples, respectively. Considering that both the absorption and scattering efficiencies are very small for small particles, the optical properties are also determined by the particles of the larger mode. (Here we note that the mass absorption coefficient was calculated only for size distributions in which the relative contribution of the second mode to total volume was larger than 93%. The sizes of the particles of the second mode were similar to those determined for

ambient TB particles observed in samples from K-puszta and Southern Africa (Pósfai et al, 2004)).

The EDS spectra of the particles generated from both the aqueous and oily phase indicated that the particles consist predominantly of carbon and oxygen. In the case of the particles formed from the aqueous phase the average carbon to oxygen molar ratio was 10:1, with 90 mol % C (RSD=10%), 9 mol % O (RSD=16%) and N, Na, Si, S, K only in trace amounts. The limitations of determining molar ratios by this method are described in detail elsewhere (Pósfai et al., 2003). It should be noted that the spectra were practically indistinguishable from those obtained from atmospheric TBs. Both HRTEM images and electron diffraction confirm that the particles in both samples are perfectly amorphous, lacking even the short-range order that is characteristic of nanosphere-soot (ns-soot) (Buseck et al., 2014).

2 Measurement uncertainties

In order to estimate the measurement uncertainties, nigrosin dye (Sigma-Aldrich, Acid black 2, water soluble) was measured with the same setup that was used for the measurements of TBs. The nigrosin was also dissolved in methanol and particles were generated with the process used for the TB samples. Oven temperature was set to 65°C in order to evaporate methanol from the droplets without inducing compositional changes of nigrosin. Using inverse Mie calculation (Guyon et al., 2003, Hoffer et al., 2006) the index of refraction of nigrozin was obtained and compared to that reported in the literature Pinnick et al., 1973). It should be noted that many parameters might affect the results of an inverse Mie calculation. Beside the uncertainty of the optical instruments, the uncertainty of the size distribution measurement (the distribution was measured as a function of electromobility diameter), as well as the experimental conditions (e.g. the presence of volatile compounds) might also contribute to the overall uncertainty of the calculations. For example, according to Massoli et al. (2009), the scattering coefficient of absorbing particles with single scattering albedo (SSA) =0.4 (at 532 nm) is overestimated by 25% using the Anderson and Ogren correction (Anderson and Ogren 1998) for the raw data measured by a TSI nephelometer. Since in our case the SSA of the generated nigrosin was ~0.4 at 550 nm, the scattering coefficient might be also overestimated by ~25%. The uncertainty of the measurements of Particle Soot Absorption Photometer (PSAP) whose measurement principle is very similar to that of the CLAP is 20–30% (Bond 1999). It was demonstrated that the presence of organic compounds

(secondary organic aerosol, SOA) causes positive bias and enhances the uncertainty of the PSAP (Cappa et al., 2008; Lack et al., 2008).

When the measured absorption and scattering coefficient of nigrosin was decreased by 25%, we obtained a refractive index of 1.65−0.29i and 1.77−0.27i for nigrosin at wavelengths of 550 and 652 nm, respectively. In this case the real part of nigrosin is slightly overestimated, as the index of refraction of nigrosin at 633 nm was reported to be 1.67−0.26i (Pinnick et al., 1973). By assuming that the absorption is similar at both 633 and 652 nm, Mie calculations using the refractive index of nigrosin (1.67−0.26i) and the measured size distribution yield scattering and absorption coefficients at 652 nm higher by ~17% and lower by ~2 %, respectively, as compared to those directly measured and corrected by 25%. These uncertainties are considered when interpreting the results. It is important to note that discrepancies in an inverse Mie calculation are a consequence of many parallel effects, thus our obtained biases might not always and generally apply.

3 Mass absorption coefficient

Table 1 summarizes the measured optical properties of the particles produced from the aqueous phase. At 650°C the measured mass absorption coefficients of the TBs generated from the aqueous phase of the wood tar varied between 2.4 and 3.2 $m^2g^{-1}C$, the average being 2.7 $m^2g^{-1}C$ at 550 nm. Taking into account the potential positive bias in absorption measurements (see discussions in Section 2) and related uncertainties (e.g. uncertainty of total carbon measurements) and the fact that the mass-to-carbon ratio of TBs is about 1.2 this range translates into mass absorption coefficients of about 0.8−3.0 m^2g^{-1} (see table 1). These values are somewhat lower (by a factor of 2–10) than that characteristic for BC (~7 m^2g^{-1}, Schnaiter et al. 2003; Clarke et al., 2004; Taha et al., 2007), but definitely much higher (by a factor of 25–100) than the mass absorption coefficient of HULIS (~0.032 m^2 g^{-1}, Hoffer et al., 2006).

The range of the measured mass absorption coefficients for the particles generated from the oily phase of wood tar was found to be largely similar to that obtained for the particles from the aqueous phase. However, the former is not evaluated since the particles generated from the oily phase morphologically differ from atmospheric TB particles.

4 Ångström exponent of generated tar balls

The absorption Ångström exponents of particles generated varied between 2.7 and 3.7 (2.7–3.4 and 3.1–3.7 for the aqueous and oily phase, respectively) in the spectral range between 467–652 nm. The Ångström exponents of the particles being closest to atmospheric TB particles in all of their observed properties are in the lower part of this range. These values are in line (but slightly lower) with those derived from laboratory observations (2.3–2.8 and 4.2–6.4 in the spectral range of 532–780 nm and 405–532 nm, respectively; Chakrabarty et al., 2010) but are markedly higher than that calculated for individual carbon spheres based on measured electron energy-loss spectra (Alexander et al., 2008). Since the AAE depends on particle size, we estimated the AAE of the brown spheres investigated by Alexander et al. (2008) and that of our laboratory generated tar balls, assuming the same size distribution. For the calculations we used the size distribution of ambient tar ball particles measured by TEM in a rural background station (K-puszta) in Hungary (Pósfai et al., 2004), as well as the reported index of refractions (at 467 and 652 nm) of the brown spheres studied by Alexander et al. (2008) and those of the tar balls generated in the present study (see section 5). The AAE of the laboratory generated TB with an ambient size distribution was 2.4 in the wavelength range between 467 and 652 nm. This value is higher than that obtained for the brown spheres (1.3) in the same wavelength range. The lack of highly ordered structures in laboratory-generated TB particles as observed by HRTEM, and the carbon-to-oxygen ratios measured by EDS reasonably explain the obtained Ångström exponents. These values fall between those of BC and humic-like substances, the less polar fraction of the water soluble fraction of the aerosol (Hoffer at al., 2006).

Tóth et al., (2004) showed that heat shock is necessary to generate TB particles from the liquid condensate obtained from biomass pyrolysis. Since the heat affects the composition and therefore the optical properties of the generated particles, investigation of the effect of temperature used for heat shock is important. The optical properties of the generated TB particles were measured continuously while the tube furnace was gradually cooled from the temperature of ~650°C (Figure 4). In the case of particles generated from the aqueous phase of the tar the Ångström exponent did not change significantly down to about 550°C, below which it drastically increased. The same phenomenon was observed for particles generated from the oily phase, the Ångström exponent (and also the SSA, not shown in the figure) changed rapidly only below a certain oven temperature (<580°C). This finding implies that the optical properties of tar balls are markedly different from those of the bulk tar material, and suggests that the chemical transformations induced by heat shock or atmospheric ageing

that produce rigid and refractory spherical particles also significantly alter the absorption properties of the resulting TB particles. The results of Mie calculations (assuming monodisperse size distribution and using the index of refraction of TBs derived for different wavelengths) showed that the AAE of the generated particles decreases with increasing particle diameter above ~150 nm. This means that the observed effect (the increasing AAE with decreasing temperature) cannot be the consequence of increasing particle size.

5 Index of refraction of tar ball particles

The indices of refraction of particles generated from the aqueous phase and aged at 650°C were calculated based on the method of Guyon et al. (2003), also used in Hoffer et al. (2006). Since the SSA of TB samples varied between 0.4 and 0.5 (at 550 nm) the measured absorption and scattering coefficients were corrected as described for the nigrosin particles. The obtained index of refraction was 1.94−0.21i (at 550 nm). Based on the nigrosin measurements, if we assume that the measured scattering coefficient is overestimated by a further 17%, the real part of the obtained index of refraction can be considered as an upper limit, as it is overestimated by about 5 %, the average value is 1.84-0.21i at 550 nm. This is comparable to the complex refractive index of individual carbon spheres—in particular in its imaginary part—calculated from TEM-electron energy loss spectra (Alexander et al., 2008). The real part of the index of refraction as measured in our experiment is higher by about 10 % than the one calculated for the carbon spheres. Assuming that the same correction applies at other wavelengths as well, the obtained average index of refraction at 467 and 652 nm is 1.84–0.27i and 1.82–0.15i, respectively.

6. Conclusions

Tar balls have been shown to be abundant in the troposphere impacted by biomass smoke which is now the main global source of anthropogenic aerosol particles. Given the abundance of TBs in the global troposphere and their relatively high absorption efficiency over the entire solar spectrum (the obtained AAE between 467–652 nm is 2.7–3.4), their contribution to column absorption can be clearly significant. This is particularly true for immense geographical regions impacted by Atmospheric Brown Clouds (ABCs) where TBs may make a contribution to solar absorption comparable to that of BC. The last question that remains is

where TBs are positioned in the black-to-brown carbon continuum of atmospheric aerosols (Andreae and Gelencsér, 2006; Sun et al., 2007). Somewhat surprisingly, their optical properties (the obtained mass absorption coefficient is 0.8–3.0 m^2g^{-1} at 550 nm) suggest that they are not very far from BC or amorphous carbon, despite their markedly different formation mechanism and chemical composition. On the other hand, it is clear that TBs are very much different from faintly coloured species such as HULIS or SOA in their absorption properties. We suggest that TBs are on the dark side of brownness of aerosol carbon, but clearly out of the BC regime both in terms of their key absorption parameters (e.g. refractive index, the obtained value is 1.84–0.21i at 550 nm and AAE) and for lack of fundamental BC properties (Petzold et al., 2013). Nevertheless, the importance of TBs in the global radiation budget is unquestionable and warrants further modelling and observational studies.

Acknowledgements

The authors thank to NOAA ESRL laboratory especially John Ogren, Betsy Andrews, and Derek Hageman for their support in data management. We also thank Pasi Aalto and the University of Helsinki for the size distribution measurements. This article was published in the framework of project TÁMOP-4.2.2.A-11/1/KONV-2012-0064 ″Regional effects of weather extremes resulting from climate change and potential mitigation measures in the coming decades″. The project was accomplished with the support of the European Union, and included co-funding from the European Social Fund.

References

Adachi, K. and Buseck, P. R.: Atmospheric tar balls from biomass burning in Mexico, J. Geophys. Res.-Atmos., 116, D05204, doi:10.1029/2010JD015102, 2011.

Alexander, D. T. L., Crozier, P. A., and Anderson, J. R.: Brown carbon spheres in East Asian outflow and their optical properties, Science, 321, 833–835, doi:10.1126/science.1155296, 2008.

Anderson, T. L., and Ogren, J. A.: Determining aerosol radiative properties using the TSI 3563 integrating nephelometer, Aerosol Sci. Technol., 29, 57–69, 1998.

Anderson, T. L., Covert, D. S., Marshall, S. F., Laucks, M. L., Charlson, R. J., Waggoner, A. P., Ogren, J. A., Caldow, R., Holm, R., Quant, F., Sem, G., Wiedensohler, A., Ahlquist, N. A., and Bates, T. S.: Performance characteristics of a high-sensitivity, three-wavelength, total scatter/backscatter nephelometer, J. Atmos. Oceanic Technol. 13, 967–986, 1996.

Andreae, M. O. and Gelencsér, A.: Black carbon or brown carbon? The nature of light-absorbing carbonaceous aerosols, Atmos. Chem. Phys., 6, 3131–3148, doi:10.5194/acp-6-3131-2006, 2006.

Bond, T. C., Anderson, T. L., and Campbell, D.: Calibration and intercomparison of filter-based measurements of visible light absorption by aerosols, Aerosol Science and Technology, 30, 582–600, 1999.

Buseck, P. R., Adachi, K., Gelencsér, A., Tompa, É., and Pósfai, M.: Ns-soot: a material-based term for strongly light-absorbing carbonaceous particles. Aerosol Science and Technology, 48, 777-788. doi: 10.1080/02786826.2014.919374, 2014.

Cappa, C. D., Lack, D. A., Burkholder, J. B., and Ravishankara, A. R.: Bias in filter-based aerosol light absorption measurements due to organic aerosol loading: evidence from laboratory measurements, Aerosol Science and Technology, 42, 1022-1032, doi:10.1080/02786820802389285, 2008.

Chakrabarty, R. K., Moosmüller, H., Chen, L.-W. A., Lewis, K., Arnott, W. P., Mazzoleni, C., Dubey, M. K., Wold, C. E., Hao, W. M., and Kreidenweis S. M.: Brown carbon in tar balls from smoldering biomass combustion, Atmos. Chem. Phys., 10, 6363–6370, doi:10.5194/acp-10-6363-2010, 2010.

China, S., Mazzoleni, C., Gorkowski, K., Aiken, A. C., and Dubey, M. K.: Morphology and mixing state of individual freshly emitted wildfire carbonaceous particles, Nature Comm., 4, 2122, doi:10.1038/ncomms3122, 2013.

Chung, C. E., Ramanathan, V., and Decremer, D.: Observationally constrained estimates of carbonaceous aerosol radiative forcing, P. Natl. Acad. Sci. USA, 109, 11624–11629, doi:10.1073/pnas.1203707109, 2012.

Clarke, A. D., Shinozuka, Y., Kapustin, V. N., Howell, S., Huebert, B., Doherty, S., Anderson, T. Covert, D., Anderson, J., Hua, X., Moore II, K. G., McNaughton, C., Carmichael, G., and Weber, R.: Size distributions and mixtures of dust and black carbon aerosol in Asian outflow: Physiochemistry and optical properties, J. Geophys. Res., 109, D15S09, doi:10.1029/2003JD004378, 2004.

Cong, Z., Kang, S., Dong, S., Zhang Y.: Individual particle analysis of atmospheric aerosols at Nam Co, Tibetan Plateau, Aerosol and Air Quality Research, 9, 323–331, doi:10.4209/aaqr.2008.12.0064, 2009.

Fu, H., Zhang, M., Li, W., Chen, J., Wang, L., Quan, X., and Wang, W.: Morphology, composition and mixing state of individual carbonaceous aerosol in urban Shanghai, Atmos. Chem. Phys., 12, 693–707, doi:10.5194/acp-12-693-2012, 2012.

Guyon, P., Boucher, O., Graham, B., Beck, J., Mayol-Bracero, O.L., Roberts, G. C., Maenhaut, W., Artaxo, P., and Andreae, M.O.: Refractive index of aerosol particles over the Amazon tropical forest during LBA-EUSTACH 1999, J. Aerosol. Sci., 34, 883–907, doi:10.1016/S0021-8502(03)00052-1, 2003.

Hand, J. L., Malm, W. C., Laskin, A., Day, D., Lee, T., Wang, C., Carrico, C., Carrillo, J., Cowin, J. P., Collet, Jr., J., and Iedema, M. J.: Optical, physical and chemical properties of tar balls observed during the Yosemite Aerosol Characterisation Study, J. Geophys. Res.-Atmos., 110, D21210, doi:10.1029/2004JD005728, 2005.

Hoffer, A., Gelencsér, A., Guyon, P., Kiss, G., Schmid, O., Frank, G. P., Artaxo, P., and Andreae, M. O.: Optical properties of humic-like substances (HULIS) in biomass-burning aerosols, Atmos. Chem. Phys., 6, 3563-3570, doi:10.5194/acp-6-3563-2006, 2006.

Lack, D. A., Cappa, C. D., Covert, D. S., Baynard, T., Massoli, P., Sierau, B., Bates, T. S., Quinn, P. K., Lovejoy, E. R., and Ravishankara, A. R.: Bias in filter-based aerosol light absorption measurements due to organic aerosol loading: evidence from ambient

measurements, Aerosol Science and Technology, 42, 1033–1041, doi:10.1080/02786820802389277, 2008.

Maschio, G., Koufopanos, C., Lucchesi, A.: Pyrolysis, a promising route for biomass utilization, Bioresource Technology, 42, 219-231, 1992.

Massoli, P., Murphy, D. M., Lack, D. A., Baynard, T., Brock, C. A., and Lovejoy, E. R.: Uncertainty in light scattering measurements by TSI nephelometer: results from laboratory studies and implications for ambient measurements, Aerosol Science and Technology, 43:11, 1064-1074, doi:10.1080/02786820903156542, 2009.

Moosmüller, H., Chakrabarty, R. K., and Arnott, W. P.: Aerosol Light Absorption and its Measurement: A Review, J. Quant. Spectrosc. Ra., 110, 844–878, 2009.

Moosmüller, H., Chakrabarty, R. K., Ehlers, K. M., and Arnott, W. P.: Absorption Ångström coefficient, brown carbon, and aerosols: basic concepts, bulk matter, and spherical particles, Atmos. Chem. Phys., 11, 1217-1225, doi:10.5194/acp-11-1217-2011, 2011.

Niemi, J. V., Saarikoski, S., Tervahattu, H., Mäkelä, T., Hillamo, R., Vehkamäki, H., Sogacheva, L., and Kulmala, M.: Changes in background aerosol composition in Finland during polluted and clean periods studied by TEM/EDX individual particle analysis, Atmos. Chem. Phys., 6, 5049–5066, doi:10.5194/acp-6-5049-2006, 2006.

Ogren, J. A.: Comment on "Calibration and Intercomparison of Filter-Based Measurements of Visible Light Absorption by Aerosols, Aerosol Science and Technology, 44:589–591, 2010.

Petzold, A., Ogren, J. A., Fiebig, M., Laj, P., Li, S.-M., Baltensperger, U., Holzer-Popp, T., Kinne, S., Pappalardo, G., Sugimoto, N., Wehrli, C., Wiedensohler, A., and Zhang, X.-Y.: Recommendations for reporting "black carbon" measurements, Atmos. Chem. Phys., 13, 8365-8379, doi:10.5194/acp-13-8365-2013, 2013.

Pinnick, R. G., Rosen, J. M., and Hofmann, D. J.: Measured light-scattering properties of individual aerosol particles compared to Mie scattering theory, Applied Optics, 12, 37–43, 1973.

Pósfai, M., Gelencsér, A., Simonics, R., Arató, K., Li, J., Hobbs, P. V., and Buseck, P. R.: Atmospheric tar balls: particles from biomass and biofuel burning, J. Geophys. Res.-Atmos., 109, D06213, doi: 10.1029/2003JD004169, 2004.

Pósfai, M., Simonics, R., Li, J., Hobbs, P.V., and Buseck, P.R.: Individual aerosol particles from biomass burning in southern Africa: 1. Compositions and size distributions of

carbonaceous particles. J. Geophys. Res.-Atmos., 108, D13, 8483, doi: 10.1029/2002JD002291, 2003.

Schnaiter, M., Horvath, H., Mohler, O., Naumann, K. H., Saathoff, H., and Schock, O. W.: UV-VIS-NIR spectral optical properties of soot and soot-containing aerosols, J. Aerosol. Sci., 34, 1421–1444, 2003.

Sun, H., Biedermann, L., and Bond, T.: Color of brown carbon: A model for ultraviolet and visible light absorption by organic carbon aerosol, Geophys. Res. Lett., 34, 17, DOI: 10.1029/2007GL029797, 2007.

Taha, G., Box, P. G., Cohen, D. D., Stelcer E.: Black Carbon Measurement using Laser Integrating Plate Method, Aerosol Science and Technology, 41:3, 266-276, DOI: 10.1080/02786820601156224, 2007.

Tóth, A., Hoffer, A., Nyirő-Kósa, I., Pósfai, M., and Gelencsér, A.: Atmospheric tar balls: aged primary droplets from biomass burning?, Atmos. Chem. Phys., 14, 6669-6675, doi:10.5194/acp-14-6669-2014, 2014.

Table 1. Optical parameters of tar ball particles generated from the aqueous phase. The AAE is calculated between 467 and 652 nm, the MAC and the refractive indices are for 550 nm.

Sample name	Tube furnace temperature (°C)	AAE	MAC (m^2g^{-1})	Re	Im	Volume of large particles (%)
18-d1	500	3.4				59
14-d1	650	2.8	0.8–2.5	1.88	0.27	98
15-d1	650	3.4		1.79	0.15	86
16-d2	650	2.8		1.87	0.27	99
17-d1	650	2.8	1.0–3.0	1.82	0.18	93
22-d2	650	3.0	0.8–2.3			93
25-d2	650	2.7	0.8–2.3	1.84	0.17	95
20-d1	800	3.0	1.0–3.1			97
20-d2	800	3.0				96

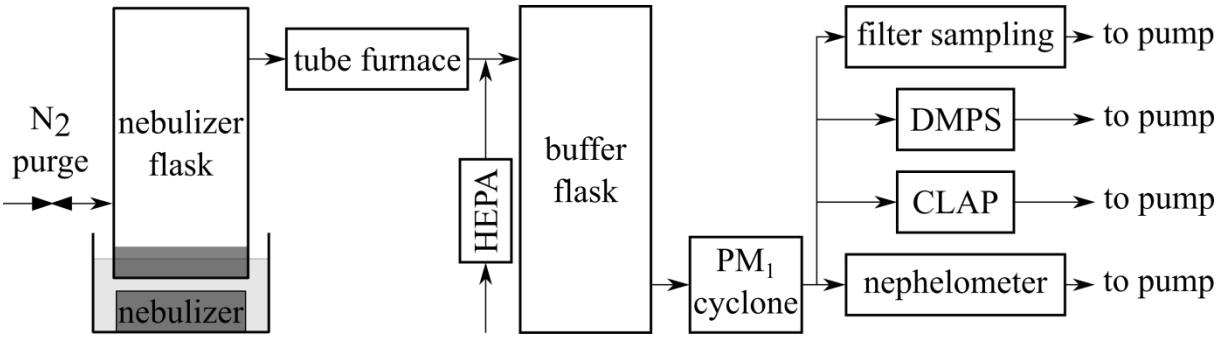

Figure 1. Experimental setup for the tar ball generation and measurement.

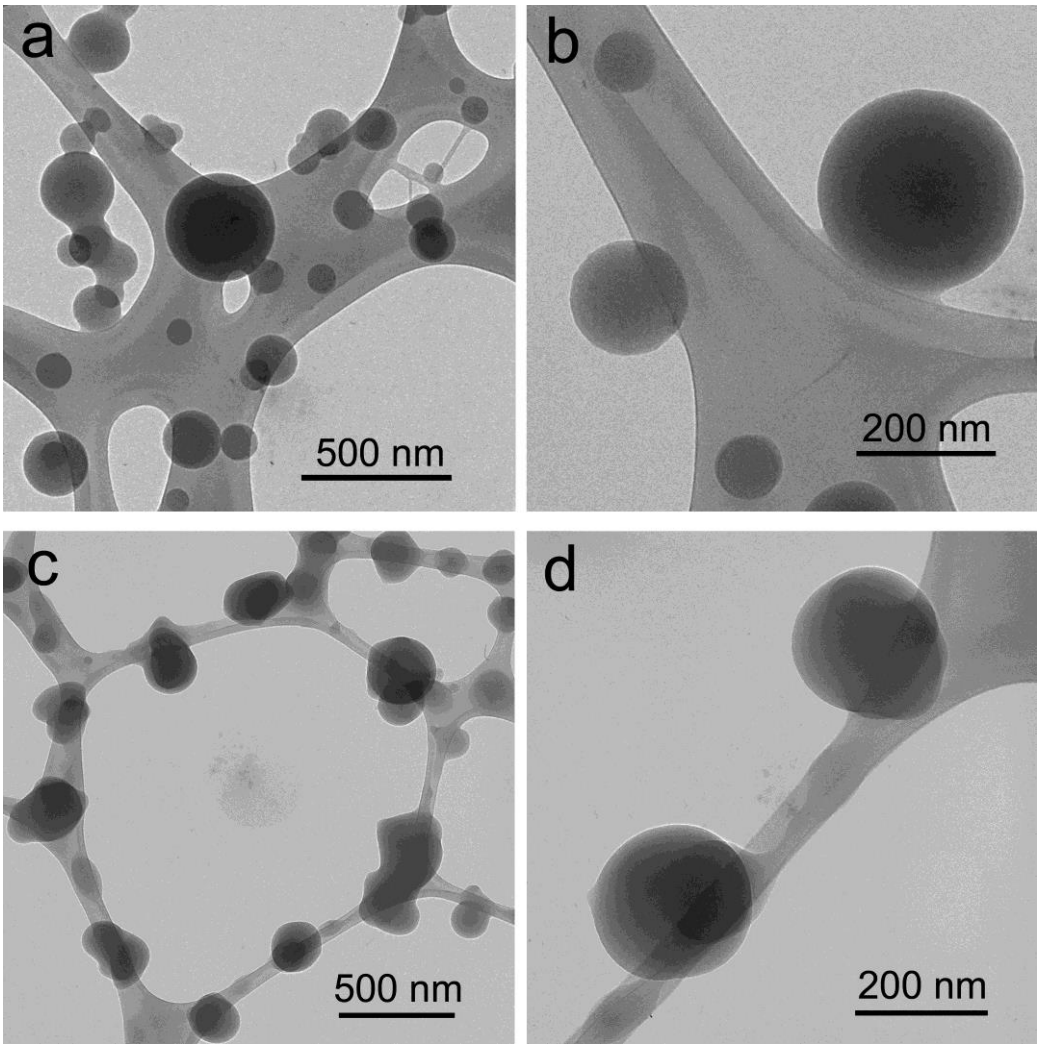

Figure 2. TEM images of tar balls generated from the aqueous (a, b) (sample 16-d2) and oily (c, d) phase of tar obtained from dry distillation of wood.

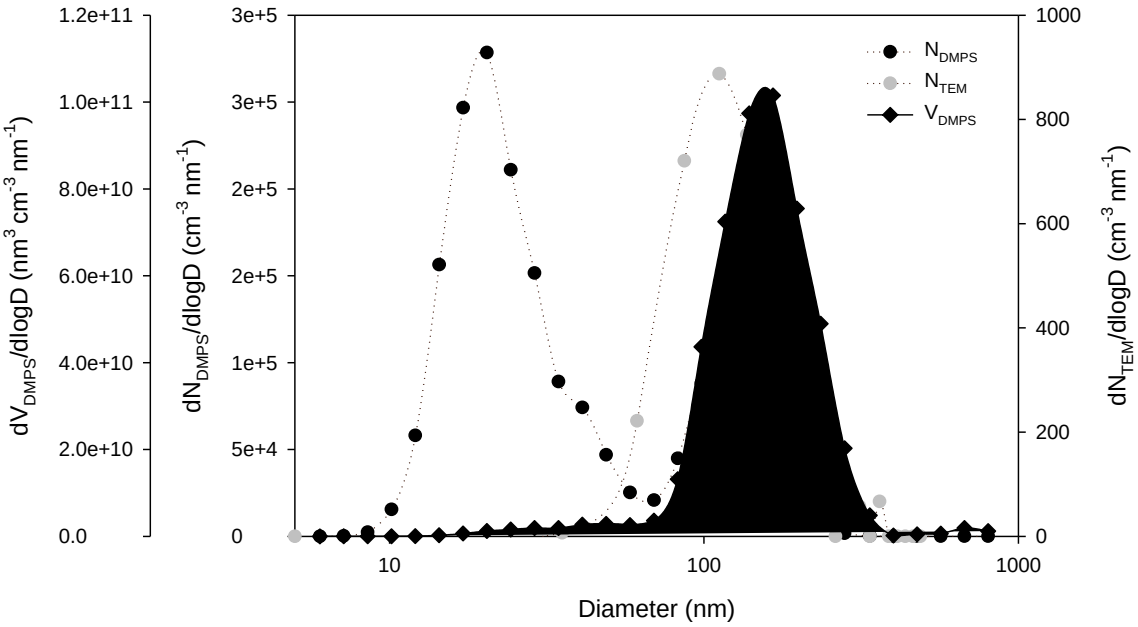

1

2

3 Figure 3. Number and volume size distribution of particles generated from aqueous tar
4 (sample 16-d2) measured with TEM and DMPS.

5

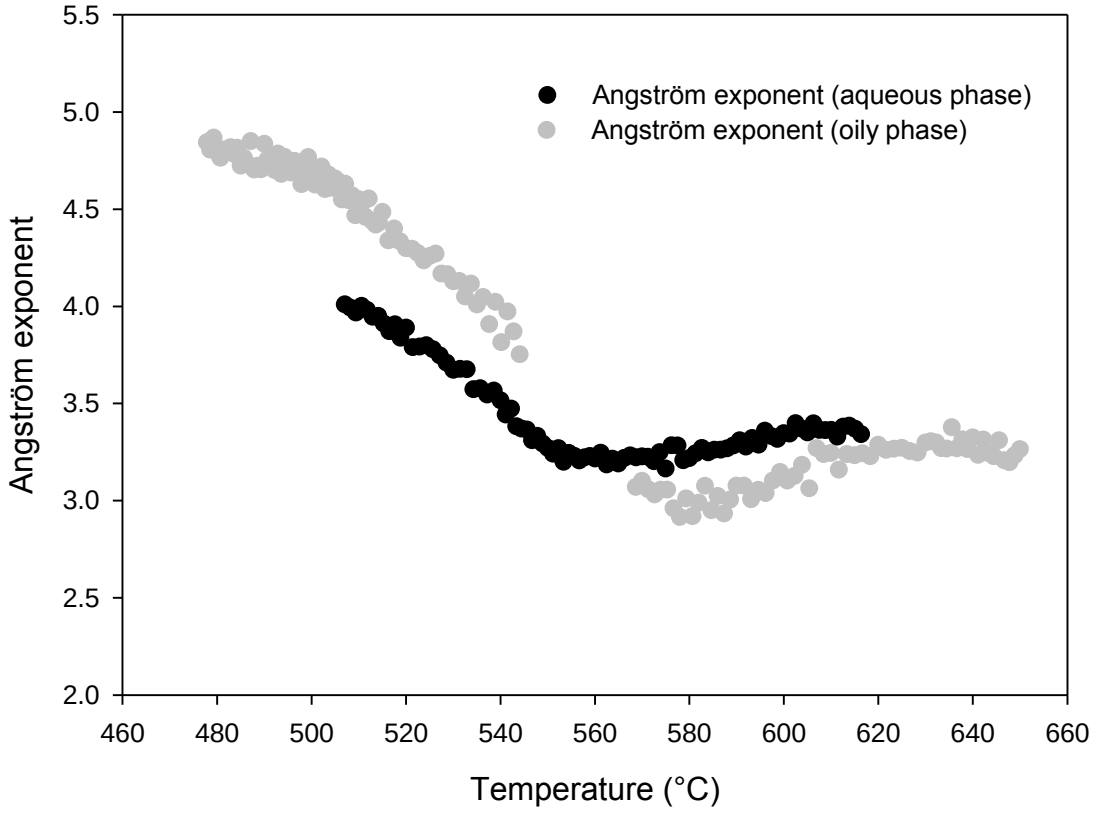

Figure 4. The effect of heat shock (oven temperature) on the Ångström exponent of TB particles generated from the aqueous and from the oily phase of wood tar.